

PAPER • OPEN ACCESS

The effect of doping variation on band gap energy and crystal structure of Biochar/TiO₂ thin layer

To cite this article: H D Fahyuan *et al* 2021 *J. Phys.: Conf. Ser.* **1731** 012060

View the [article online](#) for updates and enhancements.



240th ECS Meeting ORLANDO, FL

Orange County Convention Center Oct 10-14, 2021



Abstract submission due: April 9

SUBMIT NOW

The effect of doping variation on band gap energy and crystal structure of Biochar/TiO₂ thin layer

H D Fahyuan^{1,*}, F Deswardani¹, N Nurhidayah¹, M F Afrianto¹, H Heriansyah², N Nazaruddin³ and N Nelson⁴.

¹ Physics Study Program, Jambi University, Jambi – Ma. Bulian Street, KM 15, Mendalo Darat Jambi 36361, Indonesia

² D3 Study Program, Sains Laboratory, Bengkulu University, WR. Supratman Kandang Limun Street, Muara Bangka Hulu Bengkulu 38371, Indonesia

³ Energy and Nanomaterial Laboratory, Jambi University, Tri Brata Street, KM 11 Pondok Meja Mestong, Muaro Jambi, Indonesia

⁴ Chemistry Study Program, Jambi University, Jambi – Ma. Bulian Street, KM 15, Mendalo Darat Jambi 36361, Indonesia

*helgadwifahyuan@unja.ac.id

Abstract. The biochar/TiO₂ thin layer has been made by using the sol-gel method and the coating technique by Doctor Blade method. The variation of biochar on TiO₂ were 0%, 1%, 2%, 3% and 4%. The characterization was done by using XRD (X-Ray Diffractometer) to see the crystal structure of samples and UV-Vis spectrophotometer to obtain the value of *band gap energy*. Based on XRD data, it was obtained that the crystal structure of all samples is anatase TiO₂. The crystalline size of all samples has no significant difference by the increasing of doping percentage. The smallest crystal size was at the addition of 3% and 4% bio char which was 118.22 nm. The results of UV-Vis characterization showed the lowest value of *band gap energy* was at sample doping 1% bio char which was 3.25 eV. *Band gap energy* value for doping sample above 1% showed an increase of *band gap energy* of Biochar-TiO₂.

1. Introduction

Semiconductor material that has been observed by many researchers all over the world is TiO₂. These recent years, TiO₂ film has been extensively studied due to its interesting photocatalytic nature. TiO₂ thin film finds various applications in various fields such as photocatalysis, gas sensing, anti-reflective and protective layer, antibacterial layer and optic, dielectric film for new generation terrain effect of transistor, solar cell, etc [1].

If the thin layer of TiO₂ is applied to photocatalyst and solar cell, *band gap energy* that is wide enough from TiO₂ which is around 3,2 – 3,9 eV makes TiO₂ cannot work optimally. However, TiO₂ works effectively only at the UV wave length which means the solar energy that can be beneficial is only around 5%. Due to that reason, the modification of TiO₂ is necessary to increase the absorption of sunlight. It means, the *band gap energy* from TiO₂ must be minimized so the sunlight can be absorbed in maximum amount, and it is usually done through doping. Many doping materials that have been



used increase the TiO₂ photocatalyst performance, such as transition metal (Ti, Fe, Ru, Au, and Mo) [2-4] and non-metal (C, N, and S) [5-7].

But the problem is, those materials mentioned above are relatively expensive, non-renewable, and risky to be secondary pollutants. Getting inexpensive and eco-friendly doping that is also able to optimize TiO₂ performance need to be done. In the research, biochar made of organic waste / field waste is used as TiO₂ doping. Biochar is porous solid residue that contains rich carbon. Supported by the unique physicochemistry characteristic of biochar and its low cost, stable, eco-friendly, reachability and sustainability, biochar is the right choice as the doping for TiO₂ [8,9].

Previous research by Zhang, et al. [10] carried out photocatalyst test for TiO₂-biochar that is synthesized by using sol gel method. TiO₂-biochar showed better ability in sulfamethoxazole (SMX) than pure TiO₂. Lisowski, et al. [11] also has tested TiO₂-biochar as degradation in liquid phase and methanol selective oxidation in gas phase. The technique used in the process of Biochar/TiO₂ layer deposition is on glass substrate preparation by using *doctor blade*. *Doctor blade* is the technique used to make layers by depending on basting. This technique is used because of its simple process and low in budget.

This research is done by making layer of TiO₂ without biochar doping and with biochar doping in concentration vary between 1 to 4%. This doping is expected to be able to minimize *band gap energy* of TiO₂. The reduction of *band gap energy* can be known by using UV-Vis characterization. Based on the test of UV-Vis the value of maximum and minimum transmittance is obtained. The data are processed in *Swanepoel* equation and *Touch Plot* method to determine the *band gap energy*. And to know the structure and the size of crystal from Biochar/TiO₂, XRD (*X-ray diffraction*) analysis is executed.

2. Methods

This research took place in integrated laboratory of Science and Technology Faculty, Jambi University, Indonesia, which was started in May until August 2019. As the beginning, glass substrate preparation was cleaned in detergent solution to remove dirt like oil, dust and many more. Next, it was cleaned by using *Ultrasonic Cleaner* for 30 minutes in the alcohol 70% in order to get optimal cleaning. And the last step, glass substrate was dried by using hair drayer.

Biochar from empty bunches of palm oil, also known as *Tandan Kosong Kelapa Sawit* (TKKS) was washed, grilled, and pyrolysis by flowing it with nitrogen for 3 hours at 500 °C temperature. After the biochar got pyrolysis, the washing was done by using dionizer water (DI) to remove ash left after pyrolysis, and then it was grilled again at 80 °C temperature for two hours [12]. Next, biochar colloid/TiO₂ was made by dissolving 2 gram of pilivinil alcohol (PVA) into aquades, and then stirred by using magnetic stirrer. During the stirring process, the measuring cup was covered by using aluminium foil. The purpose is to reduce evaporation during the stirring process itself. TiO₂ powder then was added as much as 2 gram and stirred for 2 hours at 80°C temperature. At last, biochar was dissolved in 2 ml of aquades then mixed into TiO₂ colloid. It was stirred again by using magnetic stirrer for 1 hour at the same temperature [6].

TiO₂ colloid without doping and biochar/TiO₂ was deposited on preparation glass by using doctor blade technique. The colloid was dropped on the glass by using drop pipette then flattened by using glass rod until it cover up all glass surface evenly. The glass was heated up at 150°C temperature for 30 minutes to remove water vapour in the layer. Produced Biochar/TiO₂ layer was then characterized by using *ultraviolet visivel* (UV-Vis), after the maximum and the minimum transmittance values were gotten, the data were processed by using *Swanepoel* equation (equation 1) to determine the value of refractive index (equation 2), layer thickness (equation 3) and absorption coefficient (equation 4) of thin layer of Biochar/TiO₂ [13].

$$N = 2n_s \frac{T_M - T_m}{T_M T_m} + \frac{n_s^2 + 1}{2} \quad (1)$$

$$n = \sqrt{N + \sqrt{N^2 - n_s^2}} \quad (2)$$

$$d = \frac{\lambda_1 \lambda_2}{2(\lambda_1 n_2 - \lambda_2 n_1)} \quad (3)$$

$$a = -\frac{1}{d} \ln T \quad (4)$$

The next process is using *Tauc Plot* method by drawing extrapolation line at the linear area of the $h\nu$ and $(\alpha h\nu)^n$ relationship chart until it cut energy axis by using software origin that is suitable with Tauc equation (equation 5) [14].

$$(\alpha h\nu)^n = B(h\nu - E_g) \quad (5)$$

Explanation; T_M = maximum transmittance value; T_m = minimum transmittance value ; n_s = refractive index of glass ; n = refractive index ; d = layer thickness ; λ_1 = wave length 1 λ_2 = wave length 2 ; a = layer absorption coefficient; T = transmittance

XRD characterization to recognize the structure and the crystal size of Biochar/TiO₂ was done by using *Scherrer* equation (equation 6) [15].

$$D = K \frac{\lambda}{B \cos \theta} \quad (6)$$

Explanation; D is crystalline (nm), K is constant (0,96), B is graph width (Rad), λ is wave length (1,506 Å) and θ is maximum angle (Rad).

3. Results and discussion

Biochar/TiO₂ layer can be grown in glass substrate by using doctor blade technique. The layer will be white in color and spread evenly on the glass substrate. The effect of biochar doping towards the optic nature of TiO₂ can be known by using UV-Vis characterization. It was done by obtaining the transmittance value from biochar/TiO₂ layer. The sample was transmitted with 200-800 nm wave length and 50 nm in range. The range of UV is 200-400 nm while the visible is 400-800 nm. The result of transmittance measurement of biochar/TiO₂ can be seen at figure 1.

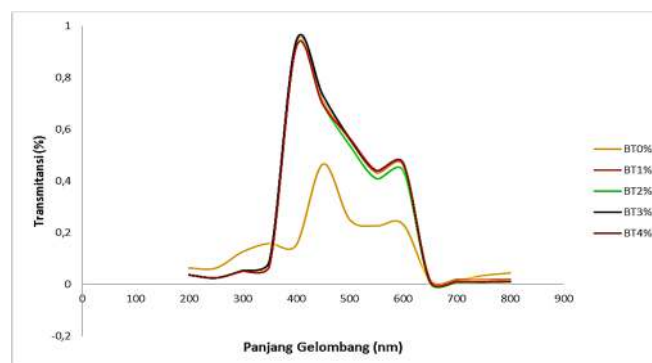


Figure 1. Transmittance of Biochar/TiO₂ layer.

From this image, it can be seen that the transmittance value of TiO₂ without biochar doping (BT0%) is lower than TiO₂ with biochar doping (BT1%, BT2%, BT3% dan BT4%), it indicates that the addition of biochar to TiO₂ increases its transmittance value. The enhancement of transmittance value shows

relatively high optical absorption at that wave length. In the other hand, the variation in biochar percentage (BT1%, BT2%, BT3% dan BT4%) did not change the transmittance value significantly. Optical transmittance value is affected by suitable doping percentage to make the bond of the structure to have fine quality, which means, biochar/TiO₂ was grown evenly and homogeny in the glass substrate. The fine quality thin layer is the layer that can transmit all visible light spectrums. In the figure 1, TiO₂ layer with biochar doping has optimal transmittance at the 400 nm wave length while without the doping, the optimal transmittance is in 450 nm wave length.

From the sample BT0%, TM_1 , TM_2 , Tm_1 , Tm_2 obtained are 0,4653; 0,2323; 0,2263; 0,1517 with the wave length 1 $\lambda_1 = 450$ and wave length 2 $\lambda_2 = 600$. From the sample BT 1% the value of transmittance increased from 0,4653 to 0,9323 with the larger range of wave length which is from 400-800 nm. The wave length that is getting larger will increase the absorption of electron of UV and visible light. It gives good impact to photocatalyst application and solar cell.

Based on transmittance spectrum of UV-Vis, the calculation of *band gap energy* is begun by using Swanepoel equation to determine the value of refractive index, layer thickness, and absorbs coefficient from biochar/TiO₂ layer [13]. The process was continued by using Tauc Plot method which is pulling extrapolation at the linear area from $h\nu$ dan $(\alpha h\nu)^n$ relationship graph until it cut energy axis [14] as shown in figure 2.

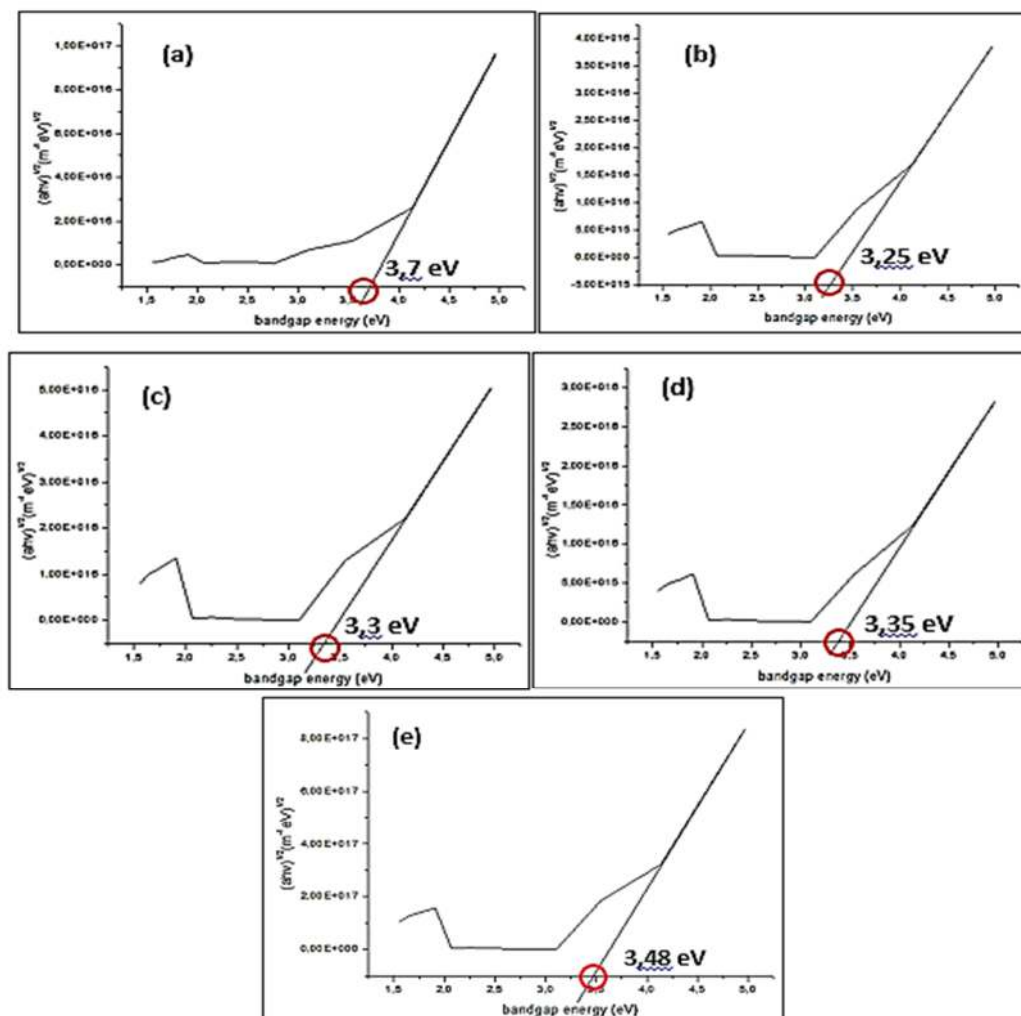


Figure 2. Bandgap energy (a) BT0% ; (b) BT1% ; (c) BT2% ; (d) BT3% ; (e) BT4%.

The figure 2 shows the relationship between band gap energy ($h\nu$) and the coefficient it was absorbed at photon ($ah\nu^2$) as the ordinate until it cut energy axis, and as the result, *band gap energy* value can be gotten. The independent variable is showed as X-axis while Y-axis shows dependent variable. The changing of the $ah\nu^2$ value is caused by the value of obtained transmittance. The smaller the value of transmittance, the bigger $ah\nu^2$ value is. The value of $h\nu$ at X-axis is affected by the wave length which is 200-800 nm. The value of *band gap energy* for all thin layers can be seen in the table 1.

Table 1. *Band gap energy* Biochar/TiO₂.

Biochar/TiO ₂ Layers	<i>Band gap energy</i>
BT0%	3,70 eV
BT1%	3,25 eV
BT2%	3,30 eV
BT3%	3,35 eV
BT4%	3,48 eV

Table 1 shows the value of *band gap energy* with the variation of biochar doping started from 0%, 1%, 2%, 3% and 4% where each is as big as 3,7 eV; 3,25 eV; 3,3 eV ; 3,35 eV and 3,48 eV. *Band gap energy* in its highest is at BT0%, while the optimal reduction of *band gap energy* happens when the doping is added as much as 1% or 3,25eV. It is caused by narrowed energy band. The narrowing itself is caused by the appearance of new energy level between valence band and conduction band after the doping. The new energy level is just a little bit above the valence band [15].

Whilst for BT2%, BT3% and BT4%, *band gap energy* increases until 3,48 eV. The increasing of *band gap energy* at 2%, 3% and 4% doping is due to the addition of doping have reached the limit of maximum ability or called doping saturation. Even though the band gap energy increases with the doping as much as 2, 3 and 4%, Table 1 shows the addition of biochar doping to TiO₂ as a whole makes the value of band gap energy TiO₂, decrease, which are 3,70 eV for BT0%; 3,25 eV for BT1%; 3,30 eV for BT2%; 3,35 eV for BT3% and 3,48 eV for BT4%. By the reduction of band gap energy, photon needed for electron excitation from valence band to conduction band will be smaller, which means electron can be transported faster and hopefully the efficiency value from the solar cell DSSC will increase, so will the photocatalyst activity.

Next step is the XRD characterization to the sample of TiO₂ without doping and biochar/TiO₂ with variation of doping, the pattern of their diffraction can be seen in the figure 3.

From the figure, five layers of biochar/TiO₂ have the peaks at 2θ around 25°, 36°, 37°, 38°, 48°, 53°, 55°, 62° and 68°, the peaks are corresponding with the peaks owned by anatase phase based on the data from JCPDS No.211272. Those peaks correspond with crystal orientation in the sector (101), (103), (004), (112), (200), (105), (211), (204), and (116). Highest peak is owned by sector orientation (101). It is shown in the figure that all pure peaks owned by anatase phase with tetragonal crystal structure, and no rutile peak appears at all. The phase of anatase crystal indicates TiO₂ has high photo catalyst nature.

Apparent crystal size from all five samples of biochar/TiO₂ layers were obtained from the data of XRD result that can be counted by using *Debye Scheerer* method, by utilizing maximum peak owned by the peak of anatase at sector orientation (101).

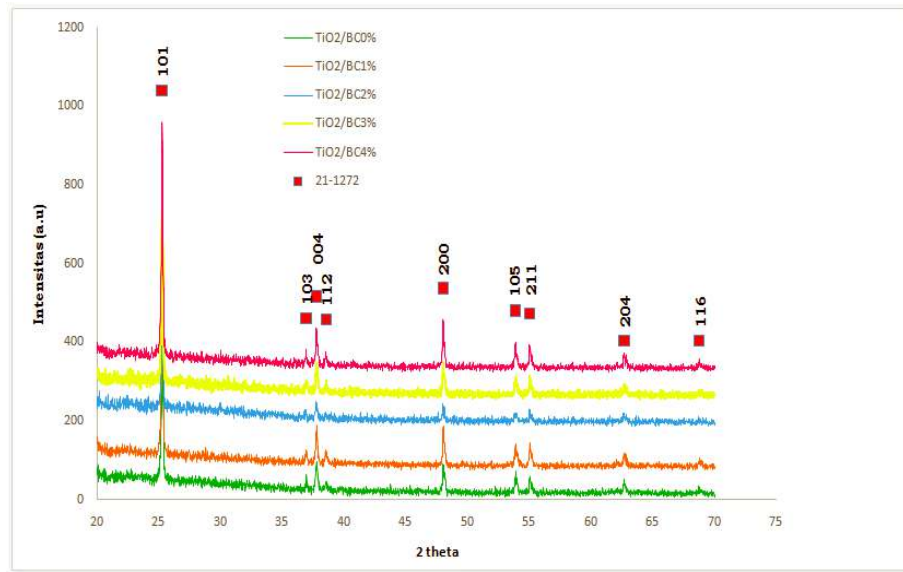


Figure 3. Diffraction pattern of Biochar//TiO₂ layers.

From the shape of the produced XRD curve profile, it can be seen that all samples have relatively same peak width which indicates the size of crystal particle is at the same order. Through quantitative calculation by using equation (6), the data about the crystal size of all five samples were obtained as shown in table 2.

Table 2. Biochar/TiO₂ crystal size.

Sample	Crystal Size (nm)
BT0%	137,95
BT1%	137,95
BT2%	137,94
BT3%	118,22
BT4%	118,22

It can be observed in the table 2 that BT0% sample produce the same crystal size as BT1% and BT2% sample which is 137,95 nm, meanwhile, BT3% sample has the same crystal size as BT4% which is 118,22 nm. Giving the right amount of doping can minimize the size of crystal of a material, but the temperature is more affecting towards the crystal size of a material. These five samples are not significantly different in size because the temperature given is same, which is 150 °C.

Small crystal will have larger surface, and it is very advantageous to be applied to DSSC solar cell and photocatalyst. Besides, the degree of samples' crystallinity are quite good as the intensity of diffraction peak is quite high and firm (Figure 3).

The fine degree of crystallinity makes the process of electron diffusion in TiO₂ to be faster, and as the implication is, the process of electron transfer for DSSC as a whole will be higher and increase the solar cell efficiency. Besides, the crystal size obtained from all five samples of Biochar/TiO₂ approach nanometer scale, so they have larger surface that can collect more dye because the smaller the crystal size is, the more cavity formed and the more dye will be absorbed which means the more photon will be absorbed too. All of this cycle as a whole increase DSSC performance.

Furthermore, anatase phase owned by biochar/TiO₂ is very advantageous when it is applied to photocatalyst. The photocatalyst activity of anatase phase is more reactive than rutile phase. The effectiveness of photocatalyst at anatase phase is caused by its larger surface so that the active side of

anatase phase per unit is bigger than the other kind of TiO₂ phase. The TiO₂ crystal with anatase phase has larger activation area, that is why it is more reactive towards light [16].

4. Conclusion

Based on this complete research, the result of *band gap energy* calculation from biochar doping towards TiO₂ is; the smallest *band gap energy* is at BT1% sample which is 3,25 eV, the doping above 1% cause the *band gap energy* of Biochar-TiO₂ increase. Moreover, the analysis of biochar-TiO₂ structure from XRD characterization shows all Biochar-TiO₂ samples are in anatase phase with tetragonal structure and the smallest size of crystal is 118,22 nm for BT3% dan BT4% samples. As a whole, the addition of biochar doping to TiO₂ can decrease the band gap energy of TiO₂, and it indicates positively if the material is applied to DSSC solar cell and photocatalyst. Besides, the other supporting factor is the material of biochar/TiO₂ is in a very stable anatase phase when it is applied to DSSC solar cell and photocatalyst.

Acknowledgments

Our gratitude is for Research and Community Service Department (*Lembaga Penelitian dan Pengabdian Masyarakat* (LPPM) of Jambi University that has given the funding for the research of Science and Technology Faculty, in 2019 fiscal year.

References

- [1] Bedikyan L, Zakhariyev S and Zakhariyeva M 2013 Titanium Dioxide Thin Film: Preparation and Optical Properties. *Jurnal of chemical tecnology and metallurgy* **48**(6) pp 555-558
- [2] Yang X, Chen W, Huang J, Zhou Y, Zhu Y and Li C 2015 Rapid degradation of methylene blue in a novel heterogeneous Fe₃O₄@rGO@TiO₂-catalyzed photo-Fenton system *Sci.Rep* **5** 10632
- [3] Kumar P, Joshi C, Labhsetwar N, Boukherroub R and Jain SL 2015 A novel Ru/TiO₂ hybrid nanocomposite catalyzed photoreduction of CO₂ to methanol under visible light *Nanoscale* **7** pp 15258–15267
- [4] Cui M, Pan S, Tang Z, Chen X, Qiao X, and Xu Q 2017 Physiochemical properties of n-n heterostructured TiO₂/Mo-TiO₂ composites and their photocatalytic degradation of gaseous toluene, *Chem. Speciation Bioavailability* **29** pp 60–69
- [5] Kalantari K, Kalbasi M, Sohrabi M, and Royaei SJ 2016 Synthesis and characterization of N-doped TiO₂ nanoparticles and their application in photocatalytic oxidation of dibenzothiophene under visible light, *Ceram. Int.* **42** pp 14834–14842
- [6] Fahyuan HD, Samsidar S, Farid F, Napitupulu S, and Pakpahan S 2015 Desain Prototipe Sel surya DSSC (Dye Sensitized Solar Cell) Lapisan Grafit/TiO₂ Berbasis Dye Alami, *Journal of Physics (JOP)* **1** pp 1 5-11
- [7] Lestari J, Fahyuan HD, and Ngatijo 2018 Pengaruh doping Al terhadap TiO₂ sebagai pendegradasi Limbah Tekstil Metyelene Blue *Journal of Physics* **3**(2) pp 15-20
- [8] Kong SH, Loh SK, Bachmann RT, Rahim SA, and Salimon J 2014 Biochar from oil palm biomass: A review of its potential and challenges *Renewable Sustainable Energy Rev.* **39** pp 729–739
- [9] Han J, Wang X, Yue J, Gao S, and Xu G 2014 Catalytic upgrading of coal pyrolysis tar over char-based catalysts, *Fuel Process. Technol.* **122** pp 98–106
- [10] Zhang H, Wang Z, Li R, Guo J, Li Y, Zhu J, and Xie X 2017 TiO₂ supported on reed straw biochar as an adsorptive and photocatalytic composite for the efficient degradation of sulfamethoxazole in aqueous matrices, *Chemosphere* **185** pp 351-360
- [11] Lisowski P, Colmenares JC, Mašek O, Lisowski W, Lisovytskiy D, Kamińska A, and Łomot D 2017 Dual functionality of TiO₂/Biochar hybrid materials: photocatalytic phenol degradation in the liquid and selective oxidation of methanol in the gas phase, *Chem. Eng.* **5**(7) pp 6274-6287

- [12] Fang C, Zhang T, Li P, Jiang RF, and Wang YC 2014 Application of Magnesium Modified Corn Biochar for Phosphorus Removal and Recovery from Swine Wastewater, *Int. J. Environ. Res. Public Health* **11** pp 9217-9237
- [13] Pimpabute N, Burinprakhon T, Somkhunthot W 2011 Determination of optical constants and thickness of amorphous GaP thin film *Optica Applicata* **XLI**(1)
- [14] Tauc J, Grigorovici R, and Vancu A 1966 Optical properties and electronic structure of amorphous germanium *physica status solidi (b)* **15**(2) 627-637
- [15] Singh AK 2005 Teknik X-Ray Tingkat Lanjut Dalam Penelitian dan Industri *Inc*, ISBN 15860353771 Linsebigler, A. L., Lu, G., & Yates Jr, J. T.
- [16] Linsebigler AL, Lu G, and Yates Jr J T 1995 Photocatalysis on surface: Principles, Mechanism and Selected Result *Chem. Rev* **95** pp 735-758